

IS THERE A MAXIMUM MASS FOR BLACK HOLES IN GALACTIC NUCLEI?

KOHEI INAYOSHI AND ZOLTÁN HAIMAN

Department of Astronomy, Columbia University, 550 West 120th Street, New York, NY 10027, USA

ABSTRACT

The largest observed supermassive black holes (SMBHs) have a mass of $M_{\text{BH}} \simeq 10^{10} M_{\odot}$, nearly independent of redshift, from the local ($z \simeq 0$) to the early ($z > 6$) Universe. We suggest that the growth of SMBHs above a few $\times 10^{10} M_{\odot}$ is prevented by small-scale accretion physics, independent of the properties of their host galaxies or of cosmology. Growing more massive BHs requires a gas supply rate from galactic scales onto a nuclear region as high as $\gtrsim 10^3 M_{\odot} \text{ yr}^{-1}$. At such a high accretion rate, most of the gas converts to stars at large radii ($\sim 10 - 100 \text{ pc}$), well before reaching the BH. We adopt a simple model (Thompson et al. 2005) for a star-forming accretion disk, and find that the accretion rate in the sub-pc nuclear region is reduced to the smaller value of at most a few $\times M_{\odot} \text{ yr}^{-1}$. This prevents SMBHs from growing above $\simeq 10^{11} M_{\odot}$ in the age of the Universe. Furthermore, once a SMBH reaches a sufficiently high mass, this rate falls below the critical value at which the accretion flow becomes advection dominated. Once this transition occurs, BH feeding can be suppressed by strong outflows and jets from hot gas near the BH. We find that the maximum SMBH mass, given by this transition, is between $M_{\text{BH,max}} \simeq (1 - 6) \times 10^{10} M_{\odot}$, depending primarily on the efficiency of angular momentum transfer inside the galactic disk, and not on other properties of the host galaxy.

Subject headings: galaxies: active — quasars: supermassive black holes — black hole physics

1. INTRODUCTION

Most massive galaxies in the local Universe are inferred to host supermassive black holes (SMBHs) with masses of $10^5 - 10^{10} M_{\odot}$ at their centers. The correlations observed between the masses (M_{BH}) of the SMBHs and the velocity dispersion (σ) and other bulk properties of their host galaxies suggest that they co-evolved during their cosmic history (e.g. Kormendy & Ho 2013, and references therein). The correlations could be caused by BH feedback, which can depress star formation and gas supply on galactic scales (e.g. Silk & Rees 1998; Fabian 1999; King 2003; Murray et al. 2005). These observations have also revealed a maximum SMBH mass of $\sim 10^{10} M_{\odot}$, in the largest elliptical galaxies (e.g. McConnell et al. 2011).

Observations of distant quasars, with redshift as high as $z \sim 7$, have found that the SMBH masses fueling the brightest quasars are similarly $\sim 10^{10} M_{\odot}$ (e.g. Fan et al. 2001; Willott et al. 2010; Mortlock et al. 2011; Wu et al. 2015). Intriguingly, this apparent maximum mass is nearly independent of redshift (e.g. Netzer 2003; Vestergaard 2004; Marconi et al. 2004; Trakhtenbrot & Netzer 2012). Since the e-folding time for BH mass growth (at the fiducial Eddington-limited accretion rate, with a 10% radiative efficiency) is $\sim 40 \text{ Myr}$, much shorter than the cosmic age. Given sufficient fuel, SMBHs could thus continue to grow, and reach masses well above $\sim 10^{10} M_{\odot}$ by $z \simeq 0$. However, we do not see SMBHs significantly above $\sim 10^{10} M_{\odot}$ in the local Universe (or indeed at intermediate redshift).

Naively, the near-constant value of the maximum SMBH mass with redshift is therefore surprising. It is tempting to attribute this observation to the same galactic-scale feedback that ties SMBH masses to their host galaxies. The maximum masses of galaxies in a fixed comoving volume are determined by the physics

of cooling and galactic feedback processes, but in general, they should increase as galaxies are assembled over time. However, local surveys probe smaller comoving volumes than high- z surveys, and can miss the rarest, most massive galaxies. In principle, this could coincidentally lead to a maximum galaxy mass that stays roughly constant with redshift. In practice, this explanation requires the $M_{\text{BH}} - \sigma$ correlation to evolve (Netzer 2003; Natarajan & Treister 2009), and also the quasar luminosity function to steepen at the bright end (Natarajan & Treister 2009).

Here we pursue a possible alternative interpretation. Namely, the observations suggest that SMBHs stopped growing at near-Eddington short after $z \simeq 5$, once they reached $\sim 10^{10} M_{\odot}$ (Trakhtenbrot et al. 2011). On the other hand, galaxies do not likewise stop their growth at this early epoch: the most massive ellipticals are believed to have assembled at $z \simeq 1 - 2$ (e.g. Bernardi et al. 2003; Thomas et al. 2005). This motivates us to hypothesize that there is a limiting mass, determined by small-scale physical processes, independent of galaxy evolution, star formation history, or background cosmology. In this paper, we discuss such a “microphysical” scenario, limiting the growth of SMBHs to a few $\times 10^{10} M_{\odot}$: disks with the high accretion rates required to produce more massive SMBHs fragment into stars. The small residual fraction of gas that trickles to the inner region is unable to form a standard geometrically thin accretion disk and to accrete onto the BH, and is instead expelled in winds or jets.¹

The rest of this paper is organized as follows. In §2, we discuss the model for star-forming accretion disks, and the implied maximum SMBH mass. In §3, we show that our results can explain the observed $M_{\text{BH}} - L_{\text{bol}}$ relation for most AGN/QSOs, as well as the maximum

¹ As this paper was being completed, we became aware of a recent preprint proposing a similar idea (King 2016). We discuss the similarities and differences between the two works in §4 below.

SMBH mass. In §4, we discuss possible caveats, and in §5 we summarize our conclusions. Throughout this paper, we define the Eddington accretion rate as $\dot{M}_{\text{Edd}} \equiv 10 L_{\text{Edd}}/c^2 = 230 M_{\odot} \text{ yr}^{-1} (M_{\text{BH}}/10^{10} M_{\odot})$.

2. LIMIT ON SMBH GROWTH VIA AN ACCRETION DISK

2.1. Star-forming accretion disks

We here consider a model for a star-forming accretion disk around a SMBH with $M_{\text{BH}} \sim 10^{8-11} M_{\odot}$ based on Thompson et al. (2005, hereafter TQM05). In this model, the gas fueling rate from galactic scales ($\gtrsim 100$ pc) to the nuclear region ($\lesssim 1$ pc) is estimated self-consistently, including gas depletion due to star-formation. Because of star-formation, the central BH is fed at a rate of $\lesssim \dot{M}_{\text{Edd}}$; this is consistent with most observed AGNs/QSOs, whose Eddington ratios are inferred to be modest (e.g. $L/L_{\text{Edd}} \sim 0.16$ for $0.35 < z < 2.25$ and $L/L_{\text{Edd}} \sim 0.43$ for $z > 4$; Shen et al. 2011; De Rosa et al. 2011). A few exceptionally bright QSOs at higher redshift are believed to accrete more rapidly, at or even somewhat above $\sim \dot{M}_{\text{Edd}}$ (see discussion in §4 below).

The TQM05 model assumes that radiation pressure from stars forming in the disk supports the gas against gravity in the vertical direction, and keeps the disk marginally stable; the Toomre parameter is then

$$Q \simeq \frac{c_s \Omega}{\pi G \Sigma_g} \simeq 1, \quad (1)$$

where c_s is the sound speed, Σ_g is the gas surface density, and Ω is the orbital frequency, given by

$$\Omega = \left(\frac{GM_{\text{BH}}}{r^3} + \frac{2\sigma^2}{r^2} \right)^{1/2}. \quad (2)$$

Here σ is the velocity dispersion characterizing the gravitational potential on galactic scales. From the continuity equation, the surface density is given by

$$\Sigma_g = \frac{\dot{M}}{2\pi r v_r} = \frac{\dot{M}}{2\pi r m c_s} \quad (3)$$

where \dot{M} is the gas accretion rate through a radius of r , v_r is the radial velocity and $m (= v_r/c_s)$ is the radial Mach number. Note that the viscosity in this model is specified by assuming a constant value of m (see below), instead of the α -prescription (Shakura & Sunyaev 1973).

The disk is supported vertically by both thermal gas pressure ($p_{\text{gas}} = \rho k_B T/m_p$) and radiation pressure due to stars in the disk, where $\rho = \Sigma_g/(2h)$ is the gas density, $h = c_s/\Omega$ is the pressure scale height and T is the gas temperature. The radiation pressure is given by

$$p_{\text{rad}} = \epsilon \dot{\Sigma}_* c \left(\frac{\tau}{2} + \xi \right), \quad (4)$$

where $\tau = \kappa \Sigma_g/2$ is the optical depth, κ is the dust opacity (Semenov et al. 2003) and $\dot{\Sigma}_*$ is the star-formation rate per unit disk surface area. The first term on the right-hand side of Eq. (4) is the radiation pressure on dust grains in the optically thick limit ($\tau \gg 1$), and the second term represents stellar UV radiation pressure and turbulent support by supernovae in optically thin limit

($\tau \ll 1$). Energy balance between cooling and heating is given by

$$\sigma_{\text{SB}} T_{\text{eff}}^4 = \frac{1}{2} \epsilon \dot{\Sigma}_* c^2 + \frac{3}{8\pi} \dot{M} \Omega^2, \quad (5)$$

where the effective temperature is given by

$$T^4 = \frac{3}{4} T_{\text{eff}}^4 \left(\tau + \frac{2}{3\tau} + \frac{4}{3} \right). \quad (6)$$

In this disk, a fraction of gas forms stars at a rate of $\dot{\Sigma}_*(r)$ and the gas accretion rate decreases inward, given by

$$\dot{M}(r) = \dot{M}_{\text{out}} - \int_{R_{\text{out}}}^r 2\pi r \dot{\Sigma}_* dr. \quad (7)$$

Eqs. (1)–(7) determine the radial profiles of all physical quantities, once the five parameters M_{BH} , σ , m , ϵ , ξ and the outer boundary conditions of the accretion rate \dot{M}_{out} at the radius R_{out} are chosen. As our fiducial model, we set $\epsilon = 10^{-3}$, appropriate for a Salpeter initial mass function (IMF) with $1 - 100 M_{\odot}$, and $\xi = 1$, appropriate when turbulent support by supernovae is negligible, as in a high- \dot{M} (or ρ) disk. The velocity dispersion is set to $\sigma = 400 \text{ km s}^{-1}$, motivated by the empirical correlation between BH mass and σ of its host galaxy for $M_{\text{BH}} \sim 10^{10} M_{\odot}$ (e.g. Tremaine et al. 2002; Gültekin et al. 2009).

We consider a very high accretion rate of $\dot{M}_{\text{out}} = 10^3 M_{\odot} \text{ yr}^{-1}$ at the boundary, in order to give a conservative estimate. From cosmological simulations (e.g. Genel et al. 2009; Fakhouri et al. 2010), the maximum gas accretion rate onto a dark matter halo is estimated as $\lesssim 10^3 M_{\odot} \text{ yr}^{-1} (M_{\text{halo}}/10^{12} M_{\odot})^{1.1} [(1+z)/7]^{5/2}$, where M_{h} is the halo mass. This could be exceeded only for brief periods during major merger events in the early Universe (Mayer et al. 2015), and for $M_{\text{h}} \gtrsim 10^{12} M_{\odot}$, gas heating by a virial shock prevents cold gas supply because of inefficient radiative cooling (Birnboim & Dekel 2003; Dekel & Birnboim 2006).

The nature of the angular momentum transfer, allowing gas to flow from large scales to the inner sub-pc regions remains uncertain. Following TQM05, we assume the transfer is provided by global density waves, and also that the radial Mach number m is constant (independent of radius). Since our results depend on the choice of m , we here consider three cases of $m = 0.05, 0.1$ and 0.2 . These values are motivated by analytical arguments yielding the limit $m \lesssim 0.2$ (Goodman 2003).

Fig. 1 shows radial profiles of the gas accretion rate (solid) and star formation rate (dashed) for three different BH masses and for $m = 0.1$. For the lowest BH mass ($M_{\text{BH}} = 10^9 M_{\odot}$; in red), star formation is inefficient at $r \gtrsim 10$ pc, and the accretion rate remains close to its value at the outer boundary. At $r \lesssim 10$ pc, vigorous star-formation depletes most of the gas, and the accretion rate rapidly decreases inward. In this domain, the disk temperature reaches the dust sublimation temperature ($T_{\text{dust,sub}} \simeq 10^3 \text{ K}$), above which the dust opacity drops rapidly. Since $\dot{\Sigma}_* \propto \Sigma_g/\kappa$ in the optimally thick limit, a high star formation rate is required to maintain the marginally-stable disk structure with $Q \simeq 1$. Within $r \lesssim 0.5$ pc, the disk becomes stable, star for-

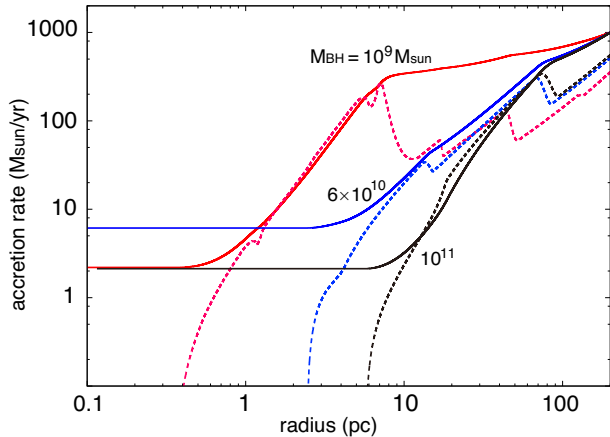


FIG. 1.— Gas accretion rate (solid) and star formation rate (dashed) in a star-forming accretion disk. The curves correspond to SMBH masses of $M_{\text{BH}} = 10^9$ (red), 6×10^{10} (blue), and $10^{11} M_{\odot}$ (black). The accretion rate at the outer boundary ($R_{\text{out}} = 200$ pc) is set to $\dot{M}_{\text{out}} = 10^3 M_{\odot} \text{ yr}^{-1}$. In each case, the accretion rate in the inner region ($\lesssim 1$ pc) approaches a constant value, which is much smaller than \dot{M}_{out} because of star-formation at larger radii.

mation ceases, and the gas accretion rate approaches a constant value. This accretion rate in the nuclear region does not depend on the value of \dot{M}_{out} , as long as $\dot{M}_{\text{out}} \gtrsim 280 M_{\odot} \text{ yr}^{-1}$ (see Eq. 44 in TQM05)², and thus hardly on the model parameters of the star-forming disk except the radial Mach number m (see §2.2). For higher SMBH masses, the accretion rate in the nuclear region gradually increases. However, for $M_{\text{BH}} \gtrsim 6 \times 10^{10} M_{\odot}$, the accretion rate at < 1 pc decreases again, because gas is depleted more efficiently due to star formation at larger radii ($r \sim 100$ pc), where evaporation of volatile organics decreases the dust opacity moderately ($T \gtrsim 400$ K) and the disk is optically thick, i.e. $\dot{\Sigma}_* \propto \Sigma_g / \kappa$.

2.2. Accretion in the sub-pc nuclear region

We next consider the stable nuclear (sub-pc) region of the accretion disk, which is embedded by the galactic star-forming disk. The properties of this disk are determined primarily by the BH mass and the gas accretion rate from larger scales ($\gtrsim 1$ pc). Fig. 2 shows the accretion rate into the nuclear region for three different Mach numbers $m = 0.05$ (blue), 0.1 (red) and 0.2 (black). Up to a turn-over at a critical M_{BH} , the accretion rates in panels (a) and (b) are fit by the single power-laws,

$$\dot{M}_{\text{BH}} \simeq 4.2 m_{0.1} M_{\text{BH},10}^{0.3} M_{\odot} \text{ yr}^{-1}, \quad (8)$$

or

$$\frac{\dot{M}_{\text{BH}}}{\dot{M}_{\text{Edd}}} \simeq 1.8 \times 10^{-2} m_{0.1} M_{\text{BH},10}^{-0.7}, \quad (9)$$

where $m_{0.1} \equiv m/0.1$ and $M_{\text{BH},10} \equiv M_{\text{BH}}/(10^{10} M_{\odot})$. This result is consistent with the analytical argument in Appendix A of TQM05³. Assuming a constant radiative

² The critical accretion rate depends on the model parameters of R_{out} , ϵ and the dust opacity at $T \lesssim 100$ K, as $280 M_{\odot} \text{ yr}^{-1} (R_{\text{out}}/200 \text{ pc})^2 (\epsilon/10^{-3})^{-1} (\kappa/10^{-3.6})^{-1}$.

³ In fact, the accretion rate (Eq. 8) depends on the dust sublimation temperature as $\dot{M}_{\text{BH}} \propto T_{\text{dust,sub}}^{3/2}$. The model of dust opacity

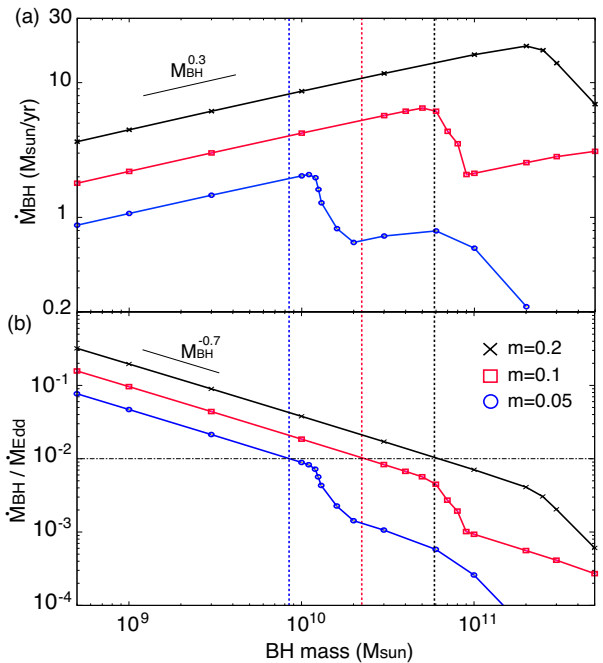


FIG. 2.— Gas accretion rate into the nuclear region (< 1 pc) as a function of SMBH mass, for three different angular momentum transfer efficiencies; $m = 0.05$ (blue), 0.1 (red) and 0.2 (black). The other parameters are the same as in Fig. 1. The horizontal line in the bottom panel marks $\dot{M}_{\text{BH}}/\dot{M}_{\text{Edd}} = 10^{-2}$, below which a thin disk changes to an ADAF (Narayan & McClintock 2008). The vertical lines mark the critical SMBH mass M_{tr} , above which the BH feeding is suppressed by strong outflows and jets.

efficiency η , we can integrate Eq. (8) over the age of the Universe and obtain $M_{\text{BH},10} \simeq 7.4 m_{0.1}^{10/7} (1-\eta)^{10/7}$. This suggests that SMBHs would not grow above $\sim 10^{11} M_{\odot}$ within the finite age of the Universe.

The above argument yields a maximum BH mass, which comes close to the largest observed masses. Here, we discuss further constraints on the maximum value, considering properties of accretion flows in the vicinity of the BH. In panel (b), the normalized rate for $M_{\text{BH}} \simeq 10^9 M_{\odot}$ is $\dot{M}_{\text{BH}}/\dot{M}_{\text{Edd}} \sim 0.1$. For this value, a standard geometrically thin, optically thick nuclear disk can form (Shakura & Sunyaev 1973). Through the disk, the BH grows via accretion at a rate given by Eq. (8). On the other hand, the normalized rate decreases with BH mass and reaches the critical value of $\dot{M}_{\text{BH}}/\dot{M}_{\text{Edd}} \lesssim 10^{-2}$, at which the nuclear disk can not remain thin, because of inefficient radiative cooling (Narayan & McClintock 2008). The inner disk would then likely be replaced by a radiatively-inefficient ADAF (advection-dominated accretion flow; Narayan & Yi 1994, 1995).⁴ Adopting the critical rate to be $\dot{M}_{\text{BH}}/\dot{M}_{\text{Edd}} = 10^{-2}$, we find that the transition occurs at $M_{\text{BH}} \gtrsim M_{\text{tr}} = 2.3 \times 10^{10} m_{0.1}^{10/7} M_{\odot}$ for $0.05 \lesssim m \lesssim 0.2$. We note that *the transition BH mass M_{tr} does not depend on the model parameters of the star-*

(Semenov et al. 2003) utilizes data on the sublimation temperature as a function of composition (Pollack et al. 1994).

⁴ Li et al. (2013) discussed a transition to a rotating accretion flow. For $\dot{M}/\dot{M}_{\text{Edd}} \lesssim 10^{-1.5}$, the rotating flow results in a solution with an even lower accretion rate and conical wind outflows.

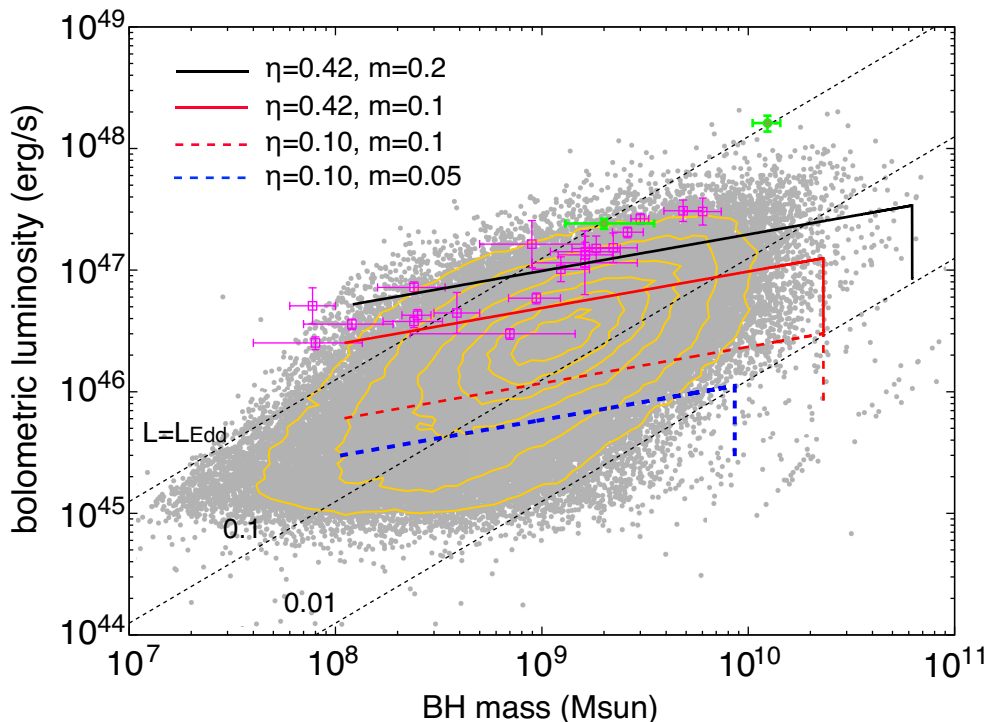


FIG. 3.— Comparison of the predicted $L_{\text{bol}} - M_{\text{BH}}$ relation with observational data. The data are taken from the AGN/QSOs samples in Shen et al. (2011) for $0 < z < 5$ (gray dots) and from several other studies for $z > 5$ (magenta; Willott et al. 2010, De Rosa et al. 2011 and green; Mortlock et al. 2011, Wu et al. 2015). The orange lines shows isodensity contours of these samples. The four thick lines correspond to the $L_{\text{bol}} - M_{\text{BH}}$ relation with different radiative efficiencies $0.1 \leq \eta \leq 0.42$ and Mach numbers $0.05 \leq m \leq 0.2$. The diagonal dotted lines indicate constant Eddington ratios (L/L_{Edd}), with values as labeled in the bottom left of the figure.

forming disk, except on the Mach number m , while the behavior of the accretion rate at $M_{\text{BH}} > M_{\text{tr}}$ depends on the choices of the other model parameters.

Once the transition to an ADAF occurs, the accretion flow through the disk becomes hot because of inefficient cooling. The hot gas near the BH would launch strong outflows and jets, suppressing the feeding of the BH (e.g. Blandford & Begelman 1999). The location of the transition radius R_{tr} , inside which a thin disk turns into a hot ADAF, has been discussed by several authors (e.g. Yuan & Narayan 2014, and references therein). Although this location is uncertain, the theoretical models suggest $R_{\text{tr}}/R_{\text{Sch}} \gtrsim 300 - 10^3 [\dot{M}_{\text{BH}}/(10^{-2}\dot{M}_{\text{Edd}})]^{-q}$ ($q > 0$) for $\dot{M}_{\text{BH}}/\dot{M}_{\text{Edd}} \lesssim 10^{-2}$. This value is consistent with results obtained from fitting the spectra of observed BH accretion systems ($R_{\text{tr}} \sim 100 R_{\text{Sch}}$ for $\dot{M}_{\text{BH}}/\dot{M}_{\text{Edd}} \sim 10^{-2}$; Yuan & Narayan 2004). Moreover, numerical simulations of ADAFs suggest that the gas accretion rate decreases inward within the transition radius as $\dot{M}_{\text{BH}} \propto (r/R_{\text{tr}})^s$ (Igumenshchev & Abramowicz 1999; Stone et al. 1999; Hawley & Balbus 2002; McKinney & Gammie 2004, see also Blandford & Begelman 1999). The power-law index is estimated as $0.4 \lesssim s \lesssim 0.6$ at $2 \lesssim r/R_{\text{Sch}} \lesssim 10^4$, independent of the strength of viscosity and magnetic field (Yuan et al. 2012). For a conservative estimate, we set $s = 0.3$ and $R_{\text{tr}} = 100 R_{\text{Sch}}$ for $\dot{M}_{\text{BH}}/\dot{M}_{\text{Edd}} \leq 10^{-2}$. This reduces the BH feeding rate by a factor of $(R_{\text{Sch}}/R_{\text{tr}})^{0.3} \simeq 0.25$ from the original accretion rate at R_{tr} (Eq. 8). As a result, the BH growth time is roughly

given by $\sim 16 [\dot{M}_{\text{BH}}/(10^{-2}\dot{M}_{\text{Edd}})]^{-1}$ Gyr, and we conclude that once an SMBH reaches the critical mass of $M_{\text{BH,max}} \simeq M_{\text{tr}} \simeq (0.9 - 6.2) \times 10^{10} M_{\odot}$, it cannot gain significant mass within the Hubble time.

3. COMPARISON TO OBSERVATIONS

In the TQM05 disk model, the BH feeding rate is a function of SMBH mass (Eq. 8). We can compare the corresponding predictions for the $L_{\text{bol}} - M_{\text{BH}}$ relation (where L_{bol} is the bolometric luminosity), with observational data. For this comparison, we use AGN/QSO samples from Shen et al. (2011)⁵ for $0 < z < 5$ and from Willott et al. (2010), De Rosa et al. (2011), Mortlock et al. (2011) and Wu et al. (2015) for $z > 5$.

For simplicity, we estimate the bolometric luminosity of the nuclear BH disk assuming a constant radiation efficiency ($L_{\text{bol}} = \eta \dot{M}_{\text{BH}} c^2$) as long as the disk is thin, i.e. $\dot{M}_{\text{BH}}/\dot{M}_{\text{Edd}} > 10^{-2}$. The radiative efficiency depends on the BH spin. Although we do not have any direct measurements of the SMBH spin evolution, applying the Paczynski-Soltan (Soltan 1982) argument to the differential quasar luminosity function, Yu & Tremaine (2002) have inferred typical radiative efficiencies of $\epsilon \gtrsim 0.3$ for the brightest quasars with the most massive SMBHs ($M_{\text{BH}} \gtrsim 10^9 M_{\odot}$), consistent with rapid spin. Recently, Trakhtenbrot (2014) independently suggested that high-redshift SMBHs with $\sim 10^{10} M_{\odot}$ have rapid spin with $a \simeq 1$, based on the band luminosities in accretion disk

⁵ http://das.sdss.org/va/qso_properties_dr7/dr7.htm

models (e.g. Davis & Laor 2011). Semi-analytical models and numerical simulations have predicted that a high value of the BH spin is maintained ($a \simeq 1$) for high- z SMBHs growing via sustained accretion of cold gas (Volonteri et al. 2007; Dubois et al. 2014). Here, we consider two opposite limits for the efficiency; $\eta = 0.1$ that is often used and $\eta = 0.42$ for an extreme Kerr BH ($a = 1$).

In Fig. 3, we show the $L_{\text{bol}} - M_{\text{BH}}$ relation predicted for four different combinations of BH spin and Mach number. As explained in §2.2 above, once the BH mass exceeds the critical value M_{tr} , the normalized accretion rate falls below $\dot{M}_{\text{BH}}/\dot{M}_{\text{Edd}} < 10^{-2}$, and the BH feeding drops. Within the range of model parameters shown in the figure, the maximum BH mass is in good agreement with the observational data ($M_{\text{BH}} \lesssim \text{few} \times 10^9 M_{\odot}$), but favors high values of a and m . The bolometric luminosities are predicted to be between $\sim 10^{45} - 10^{47}$ erg s $^{-1}$, in good agreement with the values found in the AGN/QSO samples. However, the model would require a higher m to reach the luminosities of the rarest bright objects ($\sim 1\%$ of all sources) with $\gtrsim 2 \times 10^{47}$ erg s $^{-1}$ (e.g. J010013.02+280225.8; Wu et al. 2015).

We briefly note uncertainties of the inferred bolometric luminosities. The bolometric luminosity is typically estimated from the luminosity measured in a narrow wavelength range, using a constant conversion factor based on template spectra (e.g. Elvis et al. 1994; Richards et al. 2006). However, overestimates of the conventional correction factor from the optical luminosities have been discussed (Trakhtenbrot & Netzer 2012), and several studies have suggested that the bolometric correction factors depend on M_{BH} (Kelly et al. 2008) and increase with the Eddington ratio L/L_{Edd} (Vasudevan & Fabian 2007). Thus, this method to estimate L_{bol} would have intrinsic uncertainties, especially for high- z QSOs. In addition, beaming could be present, and produce overestimates of L_{bol} for QSOs with weak emission lines (e.g. Haiman & Cen 2002). Since the fraction of weak-line QSOs is higher at $z \simeq 6$ than at lower redshift (Bañados et al. 2014), the bolometric luminosities could be overestimated for these high- z sources.

4. DISCUSSION

4.1. Maximum BH mass of the brightest QSOs

Among observed SMBHs, the brightest QSOs with $\gtrsim 2 \times 10^{47}$ erg s $^{-1}$, which are inferred to have Eddington ratios near unity ($L \sim L_{\text{Edd}}$), would grow at a rate of $\sim \dot{M}_{\text{Edd}}$. In the TQM05 model we adopted, this would require a high radial Mach number ($m \gtrsim 1$). However, such a large m is unlikely to be realized by global spiral waves in a marginally stable disk $Q \simeq 1$. Instead, this rapid inflow could be triggered by a major galaxy merger, and sustained for a few dynamical timescales of a few $\times 10^7$ yr (Hopkins & Quataert 2010, 2011). After a brief burst phase, the BH feeding rate would decrease to the value given by Eq. (8). As long as these major-merger triggered inflows are sufficiently rare and brief, the SMBH masses will remain limited by the physics of the star-forming disks, as discussed in §2.2.

We next argue that BH growth at $M_{\text{BH}} \gtrsim 10^{10} M_{\odot}$ would also be suppressed by fragmentation of the nuclear disk, even at the higher accretion rates of $\sim \dot{M}_{\text{Edd}}$. In this case, the disk becomes cold and thin instead of a hot

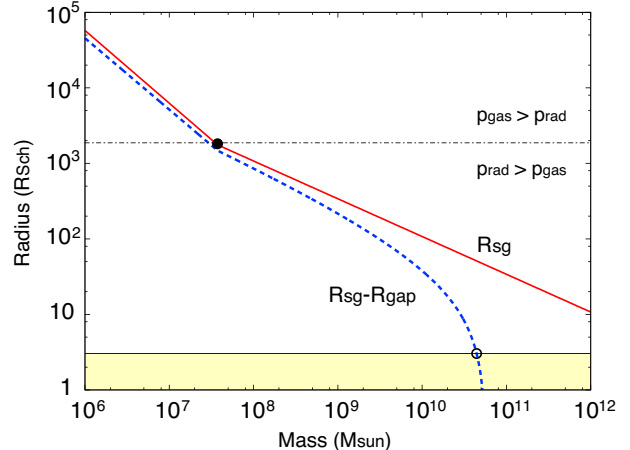


FIG. 4.— The fragmentation radius R_{sg} of a standard Shakura-Sunyaev disk in units of R_{Sch} (solid red curve) for $\alpha = 0.1$ and $\dot{M}_{\text{BH}}/\dot{M}_{\text{Edd}} = 1$. The filled circle marks the location where $p_{\text{gas}} = p_{\text{rad}}$ (with radiation pressure dominating at higher BH mass). The dashed curve shows the value of $(R_{\text{sg}} - R_{\text{gap}})$ for $f_{\text{H}} = 1.5$, where R_{gap} is the radial size of the annular gap cleared by accretion onto a clump in circular orbit at R_{sg} . At $M_{\text{BH}} = 4.5 \times 10^{10} M_{\odot}$ (open circles), a stable disk cannot exist (i.e. $R_{\text{sg}} - R_{\text{gap}} \approx R_{\text{ISCO}}$) and the BH feeding would be suppressed. We set the ISCO radius to $R_{\text{ISCO}} = 3 R_{\text{Sch}}$ (horizontal solid line).

ADAF. Such a thin disk is better described by the standard α -viscosity prescription (Shakura & Sunyaev 1973). The α -disk becomes self-gravitating and unstable at large radii, where $Q \lesssim 1$,

$$\frac{R_{\text{sg}}}{R_{\text{Sch}}} = \begin{cases} 8.1 \alpha_{0.1}^{14/27} \dot{m}_{\text{BH}}^{-8/27} M_{\text{BH},10}^{-26/27} & (p_{\text{gas}} > p_{\text{rad}}), \\ 85.3 \alpha_{0.1}^{1/3} \dot{m}_{\text{BH}}^{1/6} M_{\text{BH},10}^{-1/2} & (p_{\text{rad}} > p_{\text{gas}}), \end{cases} \quad (10)$$

where $\alpha_{0.1} \equiv \alpha/0.1$ and $\dot{m}_{\text{BH}} \equiv \dot{M}_{\text{BH}}/\dot{M}_{\text{Edd}}$ (Goodman & Tan 2004). The top (bottom) expression is valid when gas (radiation) pressure dominates. Fig. 4 shows the fragmentation radius R_{sg} as a function of the BH mass (solid curve). The filled circle marks the location where $p_{\text{gas}} = p_{\text{rad}}$, inside of which radiation pressure dominates ($M_{\text{BH}} \gtrsim 4 \times 10^7 M_{\odot}$).

Gas clumps formed in the unstable region ($r \gtrsim R_{\text{sg}}$) subsequently grow via gas accretion from the ambient disk and the gas near the clump within $\sim f_{\text{H}} R_{\text{H}}$ is depleted, where R_{H} is the clump's Hill radius and $f_{\text{H}} \sim O(1)$. Assuming that the clump grows until a density gap is created, the mass reaches a substantial fraction of the isolation mass (Goodman & Tan 2004),

$$M_{\text{c,iso}} \simeq 1.3 \times 10^9 \alpha_{0.1}^{-1/2} \dot{m}_{\text{BH}}^{5/4} M_{\text{BH},10}^{7/4} f_{\text{H}}^{3/2} M_{\odot}, \quad (11)$$

where the clump location is set to $r = R_{\text{sg}}$. The width of the gap is estimated as $R_{\text{gap}} \approx f_{\text{H}} R_{\text{H}} \approx f_{\text{H}} R_{\text{sg}} (M_{\text{c,iso}}/3M_{\text{BH}})^{1/3}$, and thus

$$\frac{R_{\text{gap}}}{R_{\text{sg}}} \approx 0.36 f_{\text{H}}^{3/2} \alpha_{0.1}^{-1/6} \dot{m}_{\text{BH}}^{5/12} M_{\text{BH},10}^{1/4}. \quad (12)$$

Fig. 4 shows the value of $(R_{\text{sg}} - R_{\text{gap}})$ for $f_{\text{H}} = 1.5$ (dashed blue curve). A stable disk can exist only below this line, down to the inner-most stable circular or-

bit (ISCO), $R_{\text{ISCO}} \simeq 3R_{\text{Sch}}$. The size of the stable region shrinks with increasing BH mass, and disappears entirely at $M_{\text{BH}} = 4.5 \times 10^{10} M_{\odot}$ (i.e. $R_{\text{sg}} - R_{\text{gap}} \approx R_{\text{ISCO}}$). Subsequently, the BH could not be fed via a stable disk. Instead, the BH could be fed stars from a nuclear star cluster, forming by the gravitational collapse of a massive clump at R_{sg} with $M_{\text{c,iso}}$. The stellar feeding occurs on the timescale of $\simeq t_{\text{relax}} \ln(2/\theta_{\text{lc}})$ (e.g. Frank & Rees 1976; Syer & Ulmer 1999), where t_{relax} is the (two-body) relaxation timescale, estimated as

$$t_{\text{relax}} \simeq \frac{0.34 \sigma_*^3}{G^2 M_{*2} \rho_* \ln(M_{\text{BH}}/M_*)} \simeq 6 \text{ Gyr}, \quad (13)$$

(Binney & Tremaine 2008; Kocsis & Tremaine 2011), where $\sigma_* = [G(M_{\text{BH}} + M_{\text{c,iso}})/R_{\text{sg}}]^{1/2}$ is the stellar velocity dispersion, M_{*2} is the ratio of the mean-square stellar mass to the mean stellar mass of the stars, and $\rho_* = 3M_{\text{c,iso}}/(4\pi R_{\text{sg}}^3)$ is the stellar density of the cluster. Assuming the Salpeter IMF with $M_{\text{min(max)}} = 1$ (100) M_{\odot} , we obtain $M_{*2} \simeq 11$ M_{\odot} . Since the angular size of the loss cone is estimated as $\theta_{\text{lc}} = \sqrt{2R_{\text{Sch}}GM_{\text{BH}}}/(\sigma_*R_{\text{sg}}) \sim 0.19$ and $\ln(2/\theta_{\text{lc}}) \sim 2.4$, the stellar feeding time for $M_{\text{BH}} > 4.5 \times 10^{10} M_{\odot}$ exceeds the age of the Universe (at $z = 0$). Therefore, we expect disk fragmentation to suppress BH growth above this mass (placing the corresponding upper limit of $L \simeq L_{\text{Edd}} \simeq 6 \times 10^{48} \text{ erg s}^{-1}$ on the luminosity).

We note that King (2016) recently proposed the existence of an upper limit on the masses of SMBHs, due to fragmentation of the nuclear disk. King (2016) suggests that the maximum mass is the one for which the fragmentation radius is located at the ISCO. This is very similar to our discussion of the case of the high- $\dot{M}_{\text{BH}}/\dot{M}_{\text{Edd}}$ α -disk above. The main difference is that King (2016) adopts a gas-pressure dominated disk, arguing that a large radiation-pressure dominated disk, extending all the way out to R_{sg} would be thermally unstable, and can not form at all. As the implications of this instability are not yet understood, we here conservatively assumed that a radiation-pressure dominated disk could still feed the central BH, as long as it is gravitationally stable. This, in principle, would greatly increase the fragmentation radius (see red solve curve in Fig. 4). However, we argued that the large physical size of the clumps in this case prevents a stable disk from forming all the way down to smaller radii, comparable to the R_{sg} in the fiducial gas-dominated case (see dashed blue curve in Fig. 4). As a result, our main conclusion agrees with that of King (2016).

4.2. $M_{\text{BH}} - M_*$ relation for the most massive BHs

In the star-forming disk model, a high accretion rate is required to feed the central BH (§2 and §3). This fact means that a large amount of stars would form around the SMBHs. We briefly discuss the stellar mass of massive galaxies hosting the most massive BHs with $\sim 10^{10} M_{\odot}$.

Fig. 5 shows radial profiles of the gas accretion rate and star formation rate for the two different values of $\dot{M}_{\text{out}} = 400$ and $10^3 M_{\odot} \text{ yr}^{-1}$ (for $M_{\text{BH}} = 10^{10} M_{\odot}$ and $m = 0.1$). We note that $\dot{M}_{\text{out}} = 400 M_{\odot} \text{ yr}^{-1}$ is sufficient to maintain the universal feeding rate in Eq.

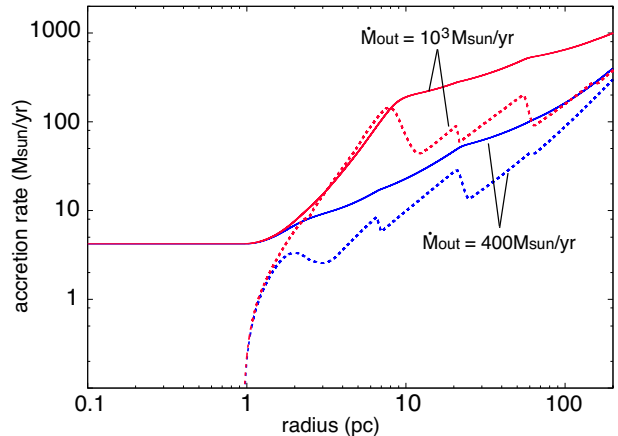


FIG. 5.— The same as Fig. 1 but $\dot{M}_{\text{out}} = 400 M_{\odot} \text{ yr}^{-1}$ (blue) and $10^3 M_{\odot} \text{ yr}^{-1}$ (red) ($M_{\text{BH}} = 10^{10} M_{\odot}$ and $m = 0.1$). For both the cases, the BH feeding rate within 1 pc is identical.

(8). In the case with $\dot{M}_{\text{out}} = 400 M_{\odot} \text{ yr}^{-1}$, a population of stars with total mass $\sim 10^{12} M_{\odot}$ forms within ~ 200 pc in the mass doubling time of the $10^{10} M_{\odot}$ BH (~ 2.5 Gyr). Note that such a compact star forming region is consistent with observed ultra-luminous infrared galaxies where stars form in a few 100 pc nuclear disk at a rate up to several $100 M_{\odot} \text{ yr}^{-1}$ (Medling et al. 2014).

The most massive elliptical galaxies are as old as $\gtrsim 8$ Gyr (e.g. Bernardi et al. 2003; Thomas et al. 2005). Thus, we can observe stars with masses of $< 1.1 M_{\odot}$, whose lifetimes are longer than the age of the galaxies (at least 8 Gyr). Although the IMF of stars around the most massive BHs is highly uncertain, many authors have discussed the possibility that stars forming in SMBH disks, including those observed in the Galactic center, have a top-heavy IMF (e.g. Paumard et al. 2006; Levin 2007; Nayakshin et al. 2007, and see also Goodman & Tan 2004). Assuming the Salpeter IMF with $M_{\text{min(max)}} = 1$ (100) M_{\odot} , 4 % of the stars in mass live in longer lifetimes of > 8 Gyr and can be observed in the most massive elliptical galaxies. Therefore, we can estimate the stellar mass surface density as $\sim 3 \times 10^{11} M_{\odot} \text{ kpc}^{-2}$, which is consistent with a maximum value of dense stellar systems within a factor of three (Hopkins et al. 2010, see also Lauer et al. 2007).

5. SUMMARY AND CONCLUSIONS

Observations of SMBHs have revealed an upper limit of a few $\times 10^{10} M_{\odot}$ on their mass, in both the local and the early Universe, nearly independent of redshift. In this paper, we have interpreted this to imply that the growth of SMBHs above this mass is stunted by small-scale physical processes, independent of the properties of their host galaxies or of cosmology. The growth of more massive SMBHs requires a high rate ($\gtrsim 10^3 M_{\odot} \text{ yr}^{-1}$) of cold gas supply from galactic scales into a nuclear region. We have argued that even if gas is supplied to the galaxy at such high rates, most of the gas forms stars at larger radii (~ 100 pc). Adopting the model by TQM05 for a star-forming disk, the accretion rate in the sub-pc nuclear region is reduced to the smaller

value of at most $\sim 4 M_{\odot} \text{ yr}^{-1} (M_{\text{BH}}/10^{10} M_{\odot})^{0.3}$. This prevents SMBHs from growing above $\simeq 10^{11} M_{\odot}$ in the age of the Universe. Furthermore, at this low rate ($\dot{M}_{\text{BH}}/\dot{M}_{\text{Edd}} \lesssim 10^{-2}$), the nuclear BH disk can not maintain a thin structure and changes to a radiatively inefficient ADAF. Once this transition occurs, the BH feeding is further suppressed by strong outflows from hot gas near the BH. The maximum mass of SMBHs is given by the critical mass where this transition occurs, $M_{\text{BH,max}} \simeq (0.9 - 6.2) \times 10^{10} M_{\odot}$, and depends primarily on the angular momentum transfer efficiency in the galactic disk, and only weakly on other properties of the host galaxy.

Although this model gives a compelling explanation for the observed maximum SMBH masses, it underpredicts, by a factor of few, the highest observed quasar luminosities. These rare high-luminosity objects would require a high (near-Eddington) accretion rate, but we have argued that they do not significantly add to the SMBH masses, because these bursts may correspond to brief

episodes following major mergers, and because we find that self-gravity prevents a stable accretion disk from forming for $M_{\text{BH}} > 4.5 \times 10^{10} M_{\odot}$ even in this high- $\dot{M}_{\text{BH}}/\dot{M}_{\text{Edd}}$ regime.

Finally, if the explanation proposed here is correct, it requires that stars forming in disks around the most massive SMBHs have a top-heavy IMF, in order to avoid over-producing the masses of compact nuclear star-clusters in massive elliptical galaxies. This is consistent with theoretical expectations.

ACKNOWLEDGEMENTS

We thank Jeremiah Ostriker, Yuri Levin, Nicholas Stone, Benny Trakhtenbrot, Kazumi Kashiyama, Shy Genel, Kohei Ichikawa and Jia Liu for fruitful discussions. This work is partially supported by Simons Foundation through the Simons Society of Fellows (KI), and by NASA grants NNX11AE05G and NNX15AB19G (ZH).

REFERENCES

- Bañados, E., Venemans, B. P., Morganson, E., et al. 2014, *AJ*, 148, 14
- Bernardi, M., Sheth, R. K., Annis, J., et al. 2003, *AJ*, 125, 1882
- Binney, J., & Tremaine, S. 2008, *Galactic Dynamics: Second Edition* (Princeton University Press)
- Birnbom, Y., & Dekel, A. 2003, *MNRAS*, 345, 349
- Blandford, R. D., & Begelman, M. C. 1999, *MNRAS*, 303, L1
- Davis, S. W., & Laor, A. 2011, *ApJ*, 728, 98
- De Rosa, G., Decarli, R., Walter, F., et al. 2011, *ApJ*, 739, 56
- Dekel, A., & Birnbom, Y. 2006, *MNRAS*, 368, 2
- Dubois, Y., Volonteri, M., & Silk, J. 2014, *MNRAS*, 440, 1590
- Elvis, M., Wilkes, B. J., McDowell, J. C., et al. 1994, *ApJS*, 95, 1
- Fabian, A. C. 1999, *MNRAS*, 308, L39
- Fakhour, O., Ma, C.-P., & Boylan-Kolchin, M. 2010, *MNRAS*, 406, 2267
- Fan, X., Narayanan, V. K., Lupton, R. H., et al. 2001, *AJ*, 122, 2833
- Frank, J., & Rees, M. J. 1976, *MNRAS*, 176, 633
- Genel, S., Genzel, R., Bouché, N., Naab, T., & Sternberg, A. 2009, *ApJ*, 701, 2002
- Goodman, J. 2003, *MNRAS*, 339, 937
- Goodman, J., & Tan, J. C. 2004, *ApJ*, 608, 108
- Gültekin, K., Richstone, D. O., Gebhardt, K., et al. 2009, *ApJ*, 698, 198
- Haiman, Z., & Cen, R. 2002, *ApJ*, 578, 702
- Hawley, J. F., & Balbus, S. A. 2002, *ApJ*, 573, 738
- Hopkins, P. F., Murray, N., Quataert, E., & Thompson, T. A. 2010, *MNRAS*, 401, L19
- Hopkins, P. F., & Quataert, E. 2010, *MNRAS*, 407, 1529
- . 2011, *MNRAS*, 415, 1027
- Igumenshchev, I. V., & Abramowicz, M. A. 1999, *MNRAS*, 303, 309
- Kelly, B. C., Bechtold, J., Trump, J. R., Vestergaard, M., & Siemiginowska, A. 2008, *ApJS*, 176, 355
- King, A. 2003, *ApJ*, 596, L27
- . 2016, *MNRAS*, 456, L109
- Kocsis, B., & Tremaine, S. 2011, *MNRAS*, 412, 187
- Kormendy, J., & Ho, L. C. 2013, *ARA&A*, 51, 511
- Lauer, T. R., Gebhardt, K., Faber, S. M., et al. 2007, *ApJ*, 664, 226
- Levin, Y. 2007, *MNRAS*, 374, 515
- Li, J., Ostriker, J., & Sunyaev, R. 2013, *ApJ*, 767, 105
- Marconi, A., Risaliti, G., Gilli, R., et al. 2004, *MNRAS*, 351, 169
- Mayer, L., Fiacconi, D., Bonoli, S., et al. 2015, *ApJ*, 810, 51
- McConnell, N. J., Ma, C.-P., Gebhardt, K., et al. 2011, *Nature*, 480, 215
- McKinney, J. C., & Gammie, C. F. 2004, *ApJ*, 611, 977
- Medling, A. M., U, V., Guedes, J., et al. 2014, *ApJ*, 784, 70
- Mortlock, D. J., Warren, S. J., Venemans, B. P., et al. 2011, *Nature*, 474, 616
- Murray, N., Quataert, E., & Thompson, T. A. 2005, *ApJ*, 618, 569
- Narayan, R., & McClintock, J. E. 2008, *New Ast. Rev.*, 51, 733
- Narayan, R., & Yi, I. 1994, *ApJ*, 428, L13
- . 1995, *ApJ*, 444, 231
- Natarajan, P., & Treister, E. 2009, *MNRAS*, 393, 838
- Nayakshin, S., Cuadra, J., & Springel, V. 2007, *MNRAS*, 379, 21
- Netzer, H. 2003, *ApJ*, 583, L5
- Paumard, T., Genzel, R., Martins, F., et al. 2006, *ApJ*, 643, 1011
- Pollack, J. B., Hollenbach, D., Beckwith, S., et al. 1994, *ApJ*, 421, 615
- Richards, G. T., Strauss, M. A., Fan, X., et al. 2006, *AJ*, 131, 2766
- Semenov, D., Henning, T., Helling, C., Ilgner, M., & Sedlmayr, E. 2003, *A&A*, 410, 611
- Shakura, N. I., & Sunyaev, R. A. 1973, *A&A*, 24, 337
- Shen, Y., Richards, G. T., Strauss, M. A., et al. 2011, *ApJS*, 194, 45
- Silk, J., & Rees, M. J. 1998, *A&A*, 331, L1
- Soltan, A. 1982, *MNRAS*, 200, 115
- Stone, J. M., Pringle, J. E., & Begelman, M. C. 1999, *MNRAS*, 310, 1002
- Syer, D., & Ulmer, A. 1999, *MNRAS*, 306, 35
- Thomas, D., Maraston, C., Bender, R., & Mendes de Oliveira, C. 2005, *ApJ*, 621, 673
- Thompson, T. A., Quataert, E., & Murray, N. 2005, *ApJ*, 630, 167
- Trakhtenbrot, B. 2014, *ApJ*, 789, L9
- Trakhtenbrot, B., & Netzer, H. 2012, *MNRAS*, 427, 3081
- Trakhtenbrot, B., Netzer, H., Lira, P., & Shemmer, O. 2011, *ApJ*, 730, 7
- Tremaine, S., Gebhardt, K., Bender, R., et al. 2002, *ApJ*, 574, 740
- Vasudevan, R. V., & Fabian, A. C. 2007, *MNRAS*, 381, 1235
- Vestergaard, M. 2004, *ApJ*, 601, 676
- Volonteri, M., Sikora, M., & Lasota, J.-P. 2007, *ApJ*, 667, 704
- Willott, C. J., Delorme, P., Reylé, C., et al. 2010, *AJ*, 139, 906
- Wu, X.-B., Wang, F., Fan, X., et al. 2015, *Nature*, 518, 512
- Yu, Q., & Tremaine, S. 2002, *MNRAS*, 335, 965
- Yuan, F., & Narayan, R. 2004, *ApJ*, 612, 724
- . 2014, *ARA&A*, 52, 529
- Yuan, F., Wu, M., & Bu, D. 2012, *ApJ*, 761, 129